17th World Conference on Earthquake Engineering, 17WCEE
Sendai, Japan - September 13th to 18th 2020

SUBSURFACE STRUCTURE BASED ON MICROTREMOR AND SEISMIC OBSERVATION IN THE OHDA AREA, SHIMANE PREFECTURE, JAPAN

T. Noguchi[(1)], I. Nishimura[(2)], T. Kagawa[(3)]

[(1)] *Assistant Professor, Tottori University, Department of engineering, nouchit@tottori-u.ac.jp*
[(2)] *Graduate student, Tottori University, Graduate School of Sustainability Science*
[(3)] *Professor, Tottori University, Department of engineering, kagawa@tottori-u.ac.jp*

Abstract

An earthquake (Mj6.1) occurred in the vicinity Ohda city western Shimane Prefecture in Japan on April 9, 2018. We conducted aftershock (strong motion) observation at several temporary sites in the area with housing damages. Characteristics of site amplification effect of the temporary sites were understood from analysis of seismic data. Also, densely microtremor observations were carried out to estimate the characteristic of ground motion in the damage area, coastal area: Hane, Kute district, Mt. Sanbe area: Shigaku district, Ohda City. Microtremor H/V spectra and a distribution of the predominant period were obtained from observation data. In addition, we checked the relationship between site effects S-wave velocities, H/V of microtremor and strong ground motion. As a result, it was found that the soft soil layers is a short period component of predominant period about 0.2-0.4 seconds may have influenced structural damage. Results of microtremor array observation are as follows. The maximum thickness of soft soil layer with Vs=80m/s to 300m/s is about 40m. The thickness of hard sedimentary layer (Vs=500m/s) was 20m to 200m, and the thickness sedimentary rock layer (Vs=700m/s - 2500m/s) was about 700m. In order to further improve the accuracy of the ground model, based on the result of microtremor analysis, the subsurface structure model was estimated from the ground motion H/V at the temporary seismic station using the diffuse wave field theory.

Keywords: microtremor observation, seismic observation, subsurface structure, characteristics of ground motion, 2018 Western Shimane prefecture earthquake

1. Introduction

An earthquake (Mj6.1) occurred in the vicinity Ohda city western Shimane Prefecture in Japan on April 9, 2018. We conducted aftershock (strong motion) observation at several temporary sites in the area with housing damages [1]. Characteristics of site amplification effect of the temporary sites were understood from analysis of seismic data. It is thought that this concentration of damage was caused by the characteristics of the strong earthquake motion, which is given by the local site effects of the area. We need to investigate the causes of the local site effects for the prevention or mitigation of earthquake disasters in the area.

The purpose of our study was to estimate the subsuface structures of the target area by using microtremor. Therefore, densely microtremor observations were carried out to estimate the characteristic of ground motion in the damage area, coastal area: Hane, Kute district, Mt. Sanbe area: Shigaku district, Ohda City. Also, the subsurface structure model was estimated from the H/V of strong ground motion at the temporary seismic station using the diffuse wave field theory based on the result of microtremor analysis.

2. Obsevation and analysis

2.1 Microtremor observation data analysis

3-compoent single-site observations at 173 points and array observations at 3 sites (RZT, KRF, KKS) were made to observe microtremor in the area (Fig.1). The array observation was executed by using many kinds of radii within the range from 0.6m to be 300m for each site according to the situation of the site.

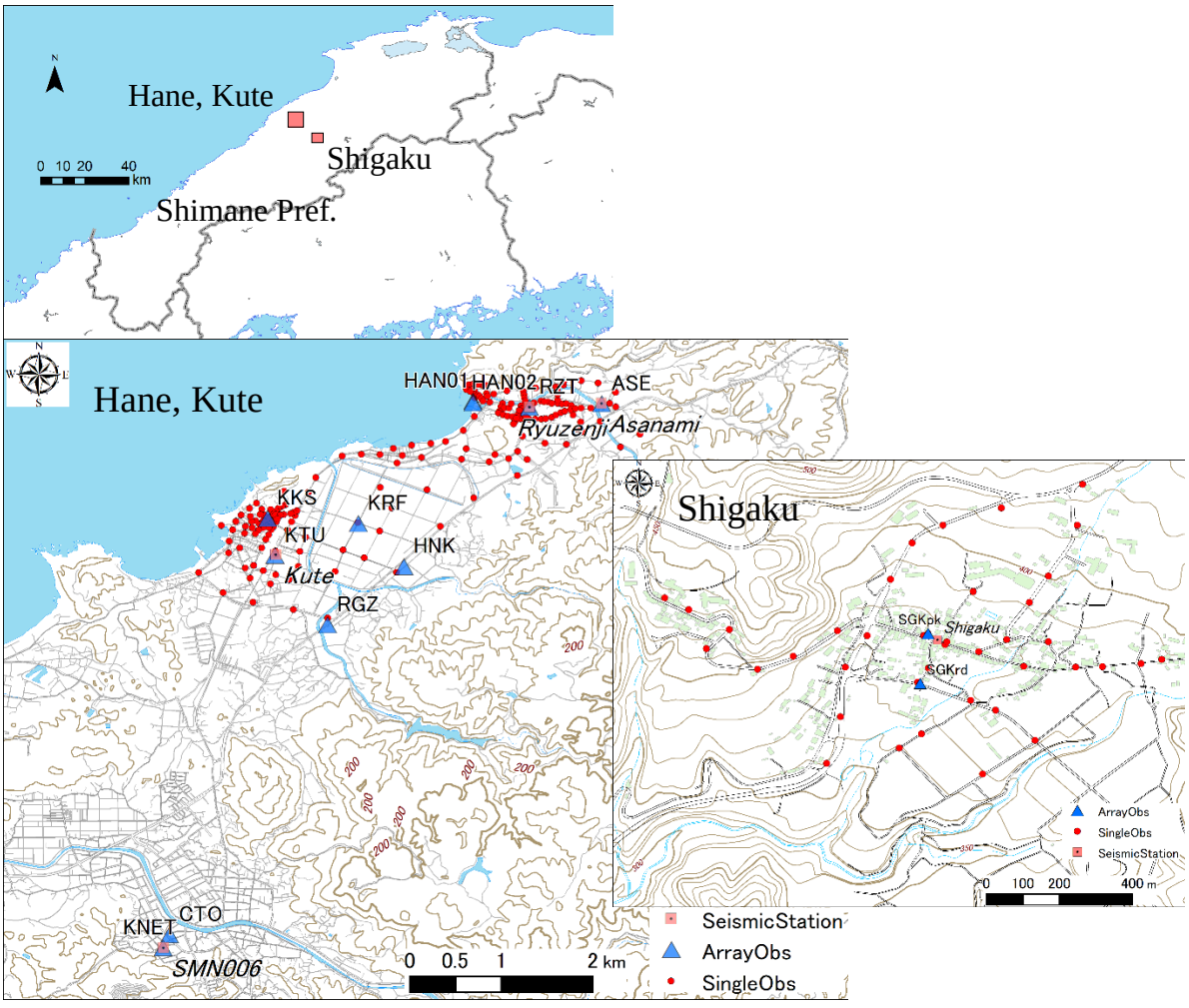

Fig. 1 – Location of observation points

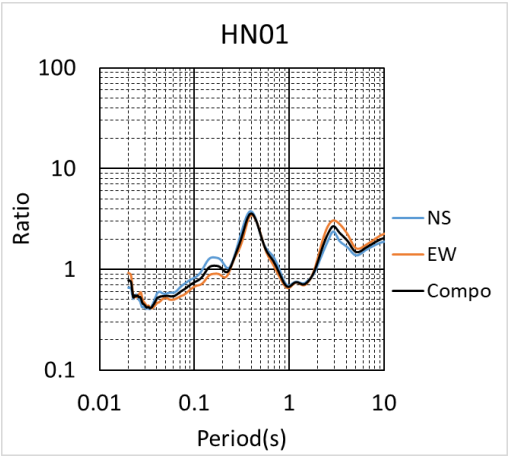

Fig. 2 – Example of H/V spectrum (Hane district)

For the analysis of the 3-componet single-site observation data, portions of 20.48s without artificial noise were selected from the array observation records. A horizontal-to-vertical spectral ratio (H/V spectrum) was calculated by using the averaged each component Fourier spectra of the selected data. Horizontal components were composed. Spectra were smoothed by a Log-window [2] with coefficient of 20.

Predominant periods of H/V were read and listed, and a distribution map of predominant periods was made by using interpolation of spline function. There are two clear peaks in H/V spectrum in the short-period band (0.2 - 0.5 s) and the long-period band (1 - 3 s). An example of H/V spectrum is shown in Fig.2.

For the analysis of the array observation data, CCA method [3] was applied and phase velocities are estimated. The CCA method are techniques of geophysical exploration that is used to infer phase velocities of surface waves using records of microtremor from a circular array of seismic sensors deployed on the ground surface. The frequency range of the dispersion curves of phase velocity are 2 - 40Hz. The minimum and maximum values of phase velocity are 80m/s and 1500m/s, respectively.

The velocity structures were determined by using a heuristic approach based on forward calculation. We determined to satisfy the phase velocity and the H/V spectrum by using fundamental mode of Rayleigh wave in the frequency range of 2 - 40Hz. Parameters of the subsurface structure models are number of layers, density, P-wave velocity; Vp, S-wave velocity; Vs, layers thickness and damping factor: P-wave; hp, S-wave; hs.

The thickness of the surface layer of the two-layer model was calculated by the following procedure. First, the S-wave velocity of the surface layer was calculated from the microtremor array subsurface structure model using a weighted average based on the layer thickness. Next, using the dominant period of H/V spectrum and S-wave velocity of surface layer, the layer thickness was calculated based on the law of quarter wavelength. The S-wave velocities for the dominant period in the short-period band were Vs=240m/s (in the Hane district), Vs=112m/s (in the Kute district) and Vs=231m/s (in the Shigaku district). The S-wave velocities for the predominant period in the long period band were Vs=670m/s (in the Hane and Kute district) and Vs=614m/s (in the Shigaku district). The predominant periods of the short and long period bands correspond to the layer thickness of the shallow and deep structures, respectively.

2.2 Seismic observation data analysis

For the seismic observation data, we use the analysis results of 5 seismic observation points (*SMN006*: K-NET station (NIDE), *Kute*, *Asanami*, *Ryuzenji*, *Shigaku*: 4 temporary station [1]) obtained in the previous study. H/V spectra were obtained from the Fourier spectrum of three components of 7 earthquake records at each point.

The subsurface structure model was estimated by inversion based on the diffusion wave field theory [4]. As the inversion method [5], a hybrid heuristic search using a genetic algorithm (GA) and an annealing method (SA) was used. The shallow structure is based on the structure model obtained by microtremor observation, and the deep structure is based on the structure model from previous studies [6]. It is expected to consider a deep ground model where enough accuracy cannot be obtained by microtremors analysis model. Furthermore, new parameters can be obtained because the attenuation is also analyzed.

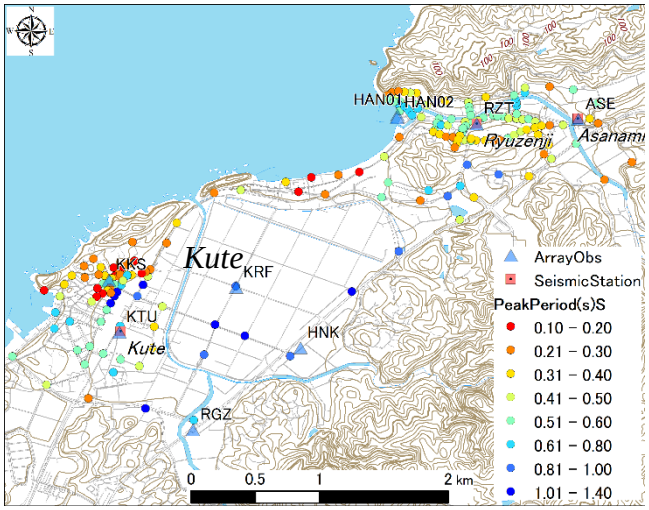

Fig. 3 – Distribution map of predominant period (Hane and Kute district, short-period band)

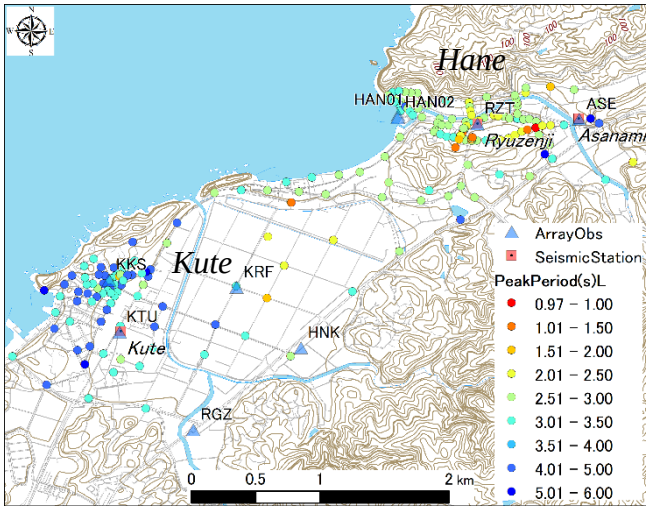

Fig. 4 – Distribution map of predominant period (Hane and Kute district, long-period band)

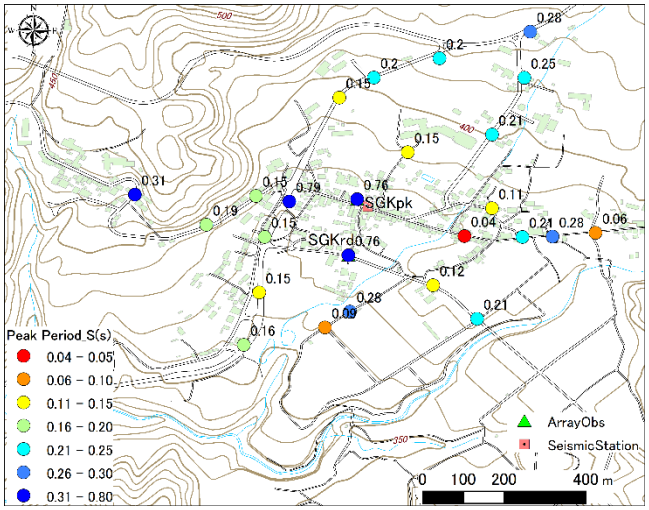

Fig. 5 – Distribution map of predominant period (Shigaku district, short-period band)

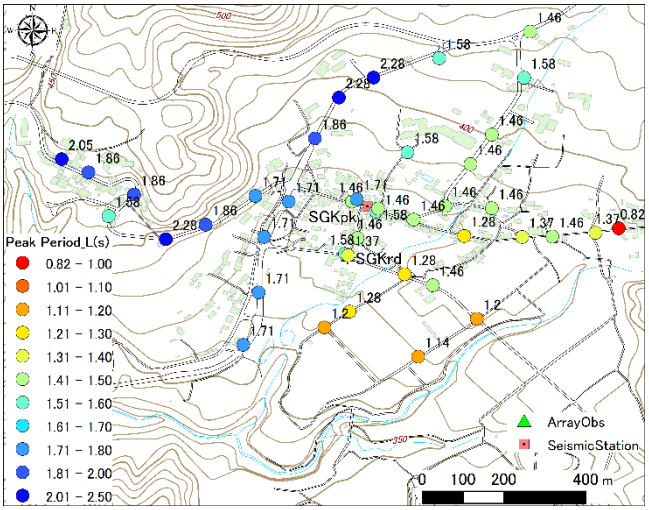

Fig. 6 – Distribution map of predominant period (Shigaku district, long-period band)

3. Subsurface structure

3.1 Predominant period

The two type distribution maps of predominant period of H/V spectra in the Hane and Kute district is shown in Fig.3 (short-period band), Fig.4 (long-period band), in the Shigaku district is shown in Fig.5 (short-period band), Fig.6 (long-period band). The feature of the predominant period distribution of the short-period band in the Hane and Kute districts are local and varied along the topography (Fig.3). The predominant periods are 0.2s - 0.6 s in the Hane area (around HAN01, HANE02, RZT, and ASE), and 0.1s - 0.2 s in the foot of the coastal mountain in Kute area (around KKS). The predominant periods of the inland plain (around KRF) are 0.8s - 1.0s in the area. The feature of the predominant period distribution of the long-period band is gently change and irrespective of the topography (Fig. 4). The predominant periods are 1.0s - 2.5s in the Hane area and 2.0s - 4.0s in the Kute area.

Table 1 – Parameter of subsurface structure model by microtremor analysis (this study)

RZT

Thickness (m)	ρ(t/m³)	Vp(m/s)	Vs(m/s)
5	1.6	1490	170
25	1.9	1570	250
150	2.1	1840	500
400	2.2	2180	800
300	2.4	2730	1300
∞	2.6	4070	2500

KKS

Thickness (m)	ρ(t/m³)	Vp(m/s)	Vs(m/s)
10	1.5	1340	80
50	1.9	1620	300
150	1.9	1850	500
400	2.1	2170	800
400	2.2	2720	1300
∞	2.5	4040	2500

KRF

Thickness (m)	ρ(t/m³)	Vp(m/s)	Vs(m/s)
28	1.3	1400	100
200	2.1	1850	500
400	2.2	2180	800
400	2.4	2730	1300
∞	2.6	4065	2500

Table 2 – Parameter of subsurface structure model by microtremor analysis (Noguchi et al. [1])

ASE

Thickness (m)	ρ(t/m³)	Vp(m/s)	Vs(m/s)
7	1.5	1460	150
15	1.7	1570	250
40	2.1	1850	500
400	2.2	2180	800
300	2.4	2730	1300
∞	2.6	4070	2500

HAN01

Thickness (m)	ρ(t/m³)	Vp(m/s)	Vs(m/s)
30	1.9	1550	220
150	2.1	1850	500
300	2.2	2180	800
400	2.4	2730	1300
∞	2.6	4065	2500

HAN02

Thickness (m)	ρ(t/m³)	Vp(m/s)	Vs(m/s)
5	1.6	1460	150
25	1.9	1550	230
150	2.1	1850	500
300	2.2	2180	800
400	2.4	2730	1300
∞	2.6	4065	2500

KTU

Thickness (m)	ρ(t/m³)	Vp(m/s)	Vs(m/s)
25	1.5	1460	150
150	2.1	1850	500
200	2.2	2180	800
400	2.4	2730	1300
∞	2.6	4065	2500

RGZ

Thickness (m)	ρ(t/m³)	Vp(m/s)	Vs(m/s)
20	1.5	1460	110
200	2.1	1850	500
400	2.2	2180	800
400	2.4	2730	1300
∞	2.6	4065	2500

HNK

Thickness (m)	ρ(t/m³)	Vp(m/s)	Vs(m/s)
26	1.5	1420	120
200	2.1	1850	500
400	2.2	2180	800
400	2.4	2730	1300
∞	2.6	4065	2500

CTO

Thickness (m)	ρ(t/m³)	Vp(m/s)	Vs(m/s)
20	1.7	1650	320
30	2.1	1910	560
100	2.2	2180	800
500	2.4	2730	1300
∞	2.6	4065	2500

KNET

Thickness (m)	ρ(t/m³)	Vp(m/s)	Vs(m/s)
4	1.5	1610	290
17	1.7	1910	560
50	2.2	2180	800
500	2.4	2730	1300
∞	2.6	4065	2500

SGKpk

Thickness (m)	ρ(t/m³)	Vp(m/s)	Vs(m/s)
40	1.9	1550	230
200	2.2	2070	700
500	2.4	2730	1300
∞	2.6	4065	2500

SGKrd

Thickness (m)	ρ(t/m³)	Vp(m/s)	Vs(m/s)
20	1.9	1480	170
23	1.9	1550	250
200	2.2	2070	700
450	2.4	2730	1300
∞	2.6	4065	2500

The feature of the predominant period distribution of the short period band in the Shigaku district is that the predominant periods become shorter as the altitude decreases from north to south (Fig. 5). Near the center of this map, there are places where the predominant periods become locally long. The predominant periods are 0.05s - 0.3 s. The feature of the long-period dominant period distribution is that the predominant periods increase from the east to the west, regardless of the topography (Fig. 6). The predominant periods are 1.0s - 2.5s.

3.2 S-wave velocity structure

The parameters of the subsurface structure models by this study are shown in Table 1, by previous studies [1] are shown in Table 2. Graphs of S-wave velocity model are shown in Fig.7 (this study), Fig.8 (previous study). The red numbers in these graphs denote the depth to the engineering basement (layer of Vs=500m/s or 700m/s). From the subsurface structure model, first, focusing on the shallow structure. There are very soft layer with S-wave velocity is less than 100m/s at 2 points and soft layer with S-wave velocity is less than 150m/s at 7 points. The maximum value of depth to the layer of Vs=500m/s is 40m. It is considered

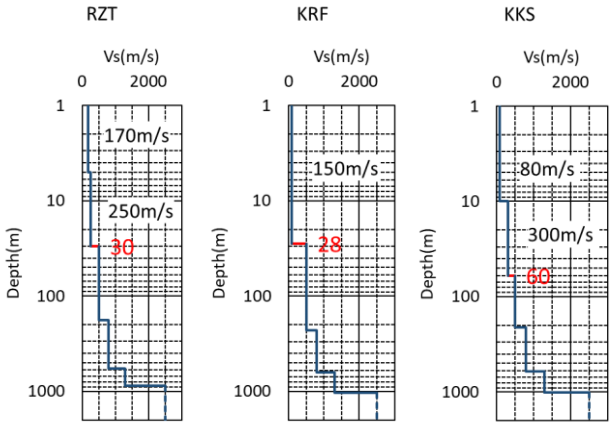

Fig. 7 – S-wave velocity structure (this study)

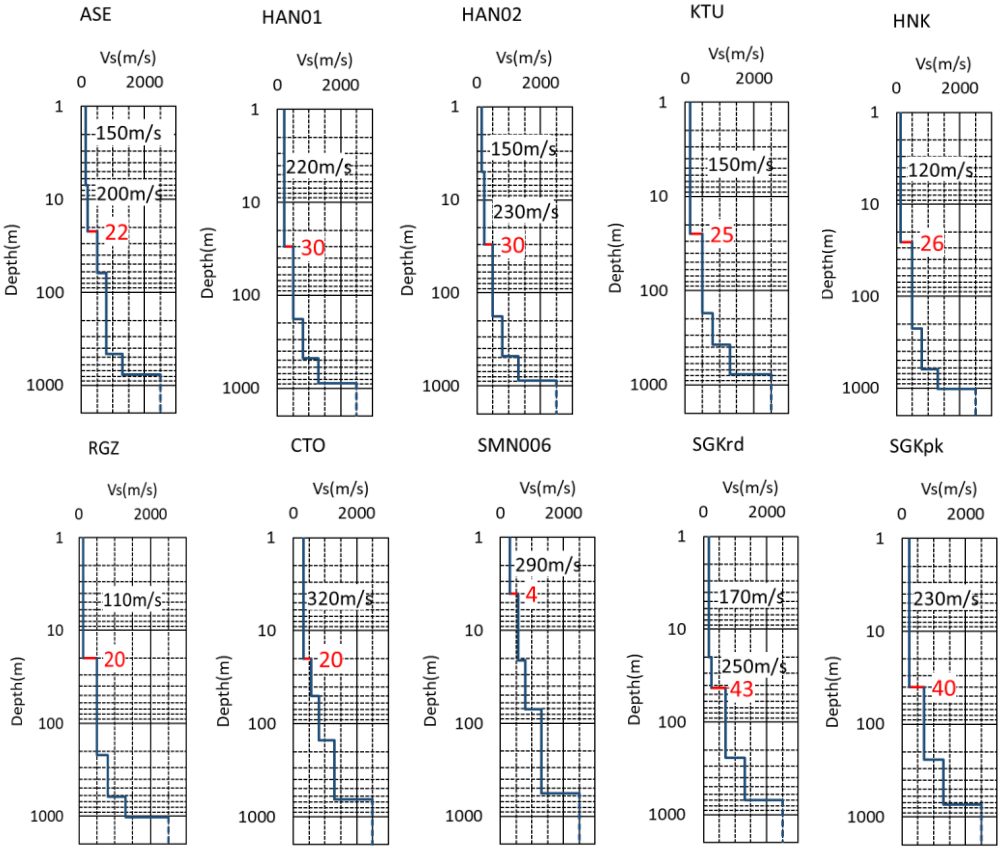

Fig. 8 – S-wave velocity structure (Noguchi et al. [1])

that the shallow subsurface structure greatly affects the site amplification. Next, focusing on the deep structure, the depth up to the layer of Vs = 2500m/s is 700-1000m, and there is no significant change in each region.

The parameters of the subsurface structure models of this analysis are shown in Table 3. H/V spectra of the earthquakes and overlaid theoretical values obtained from the subsurface models are shown in Fig.9. From the ground structure model (Table 3) based on the analysis of ground motion H/V spectrum, the layers corresponding to Vs=500m/s and Vs=800m/s in the microtremor model (Table 1 and Table 2) are thin, and the layer corresponding to Vs=1300m/s is thick. The damping factors (hp, hs) are 0.03-0.09 for the soft soil layer

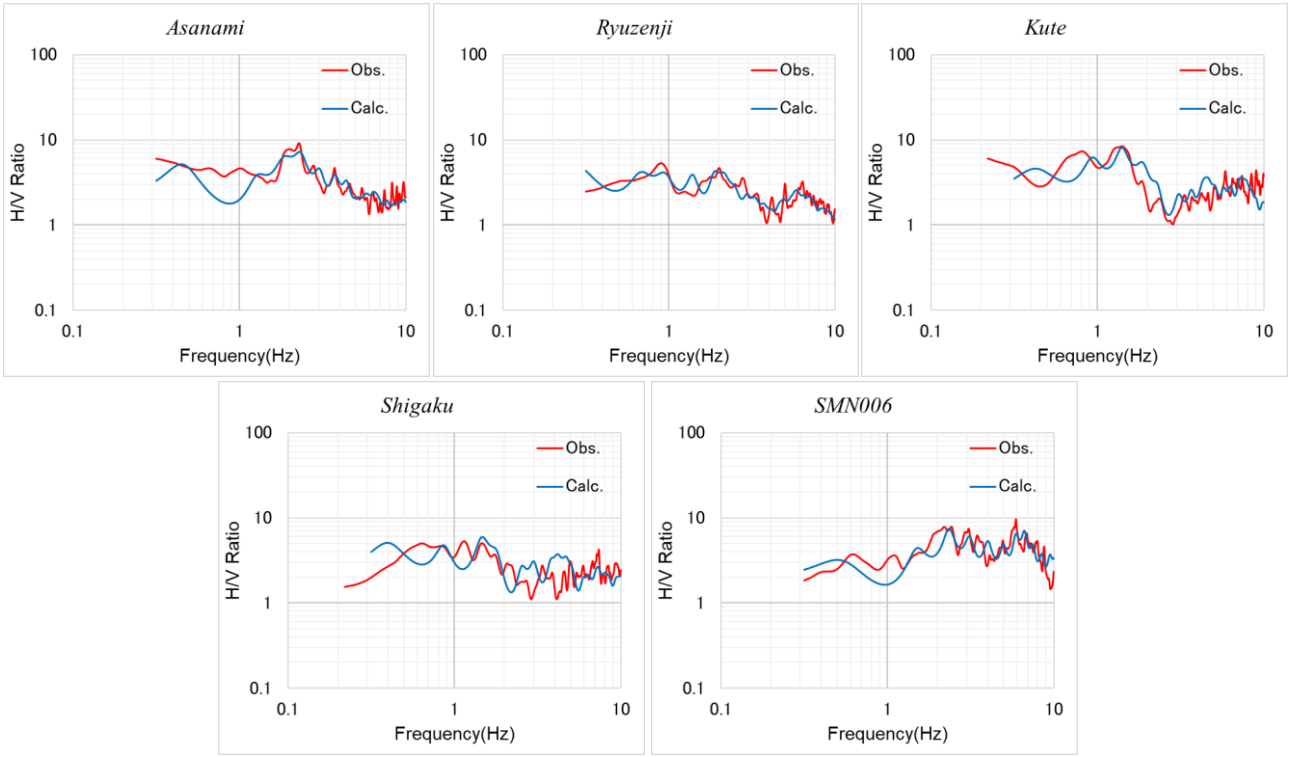

Fig. 9 – H/V spectrum of earthquake

Table 3 – Parameter of subsurface structure model by earthquake analysis

Asanami

Thickness (m)	ρ(t/m³)	Vp(m/s)	Vs(m/s)	hp	hs
7.0	1.7	1272.7	150.0	0.07	0.09
15.0	1.7	1379.5	250.0	0.06	0.08
40.5	1.9	1464.1	527.4	0.04	0.02
356.4	2.0	2583.7	855.7	0.08	0.03
192.2	2.2	2834.7	1376.2	0.05	0.02
∞	2.5	4065.0	2500.0	0.08	0.06

Ryuzenji

Thickness (m)	ρ(t/m³)	Vp(m/s)	Vs(m/s)	hp	hs
5.0	1.7	1535.8	170.0	0.06	0.04
25.0	1.7	1808.0	250.0	0.07	0.07
111.5	1.8	1971.2	433.6	0.04	0.07
509.4	2.0	2537.8	890.9	0.09	0.03
419.5	2.2	3085.3	1321.1	0.09	0.04
∞	2.5	4065.0	2500.0	0.03	0.05

Kute

Thickness (m)	ρ(t/m³)	Vp(m/s)	Vs(m/s)	hp	hs
25.0	1.7	1480.0	150.0	0.07	0.09
83.2	1.9	1532.2	542.1	0.04	0.03
185.4	2.0	2305.9	889.5	0.05	0.02
506.9	2.2	2888.3	1336.1	0.09	0.01
∞	2.5	4065.0	2500.0	0.05	0.03

Shigaku

Thickness (m)	ρ(t/m³)	Vp(m/s)	Vs(m/s)	hp	hs
40.0	1.7	1325.3	230.0	0.09	0.09
162.2	1.9	1643.4	587.6	0.08	0.03
505.9	2.1	2461.4	1123.7	0.09	0.02
∞	2.5	4065.0	2500.0	0.03	0.06

SMN006

Thickness (m)	ρ(t/m³)	Vp(m/s)	Vs(m/s)	hp	hs
4.0	1.8	1359.6	290.0	0.03	0.06
24.9	1.9	1581.8	560.0	0.03	0.02
45.7	2.0	2689.3	785.3	0.02	0.01
631.6	2.2	2981.9	1413.3	0.10	0.01
∞	2.5	4065.0	2500.0	0.04	0.05

with S-wave velocity is less than 250m/s, and 0.02-0.09 for the hard soil or rock layer with S-wave velocity of more than 500m/s.

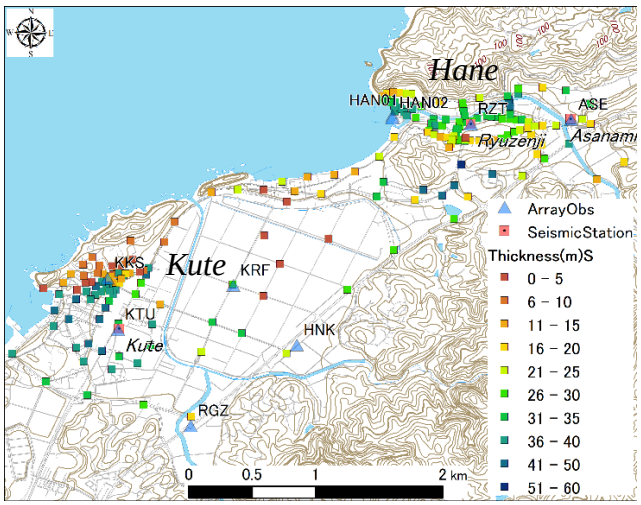

Fig. 10 – Distribution map of thickness (Hane and Kute district, shallow structure)

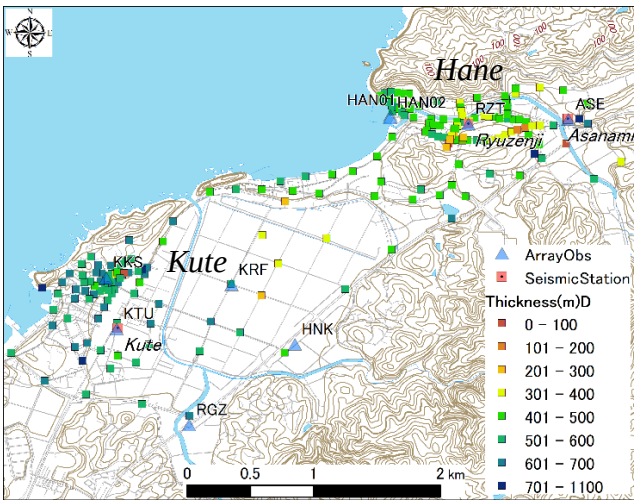

Fig. 11 – Distribution map of thickness (Hane and Kute district, deep structure)

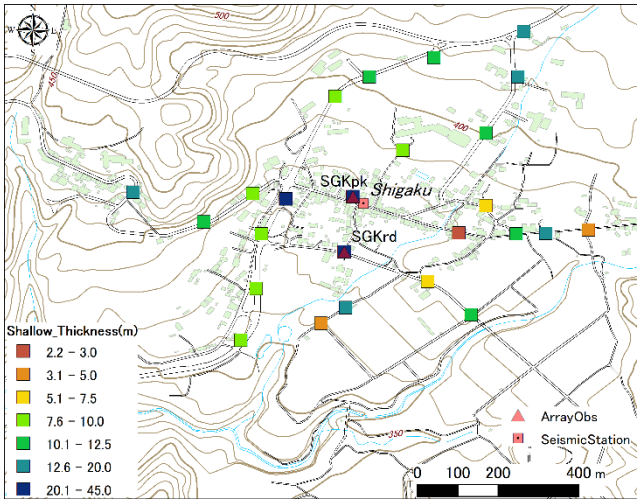

Fig. 12 – Distribution map of thickness (Shigaku district, shallow structure)

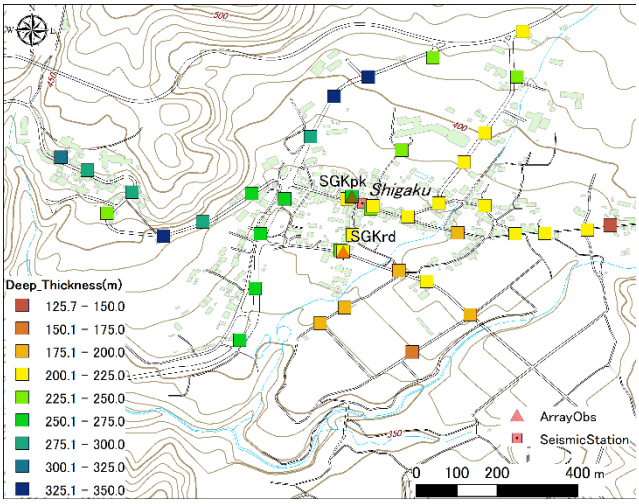

Fig. 13 – Distribution map of thickness (Shigaku district, deep structure)

3.3 Thickness of 2-layer model

The two type distribution maps of thickness of 2-layer model in the Hane and Kute district are shown in Fig.10 (shallow structure), Fig.11 (deep structure), in the Shigaku district in Fig.12 (shallow structure), Fig.13 (deep structure). The distribution of layer thickness in each district shows the same distribution feature as the predominant period distribution, the region with a long predominant period corresponds to the region with a large layer thickness. The thickness of the shallow subsurface structures in the Hane and Kute districts are about 5m -30 m in the Hane district and about 5m -50 m in the Kute district (Fig.10). The thicknesses of the deep subsurface structures are about 100m - 500m in the Hane area and about 100m - 700m in the Kute area (Fig.11). The thicknesses of the Shigaku area are 2m - 40m for the shallow subsurface structure (Fig.12) and 100m - 300m for the deep subsurface structure (Fig.13).

4. Acknowledgements

We used seismic records and PS logging information of K-NET the National Research Institute for Earth Science and Disaster Prevention. The base map of the GSI was used as the base map of the observation points and the resulting map.

5. References

[1] Noguchi, T., T. Kagawa, S. Yoshida and Y. Yamaguchi (2019): Subsurface structure and evaluation of site effects at strong ground motion observation sites in Tottori prefecture, *Journal of Earthquake Engineering, JSCE*, Vo.75, No.4, Vol.38, p.I_701-I_713 (in Japanese with English abstract).

[2] Konno, K. and T. Ohmachi (1995): A smoothing function sutable for estimation of amplification factor of the surface ground from microtremor and its application, *Journal of JSCE*, No.524/1-33, 247-259 (in Japanese with English abstract).

[3] Cho, I., T. Tada, and Y. Shinozaki (2006): Centerless circular array method: Inferring phase velocities of Rayleigh waves in broad wavelength ranges using microtremor records, *Journal of Geophysical Research*, 111, B09315.

[4] Kawase, H., F.J. Sanchez-Seama and S. Matsushima (2011): The optimal use of horizontal-to-vertiacal spectral ratios of earthquake motions for plane waves, *Bulletin of the Seismological Society of America*, Vol.101, No.5, 2001-2014.

[5] Yamanaka, H. (2007): Inversion of surface-wave phase velocity using hybrid heuristic search method, geophysical Exploration, *Butsuri-Tansa*, Vol.60, No.3, 265-275 (in Japanese with English abstract).

[6] Adachi, M., T. Noguchi, K. Omuda and R. Nishida (2009): Determination of the Underground Structure of Izumo plain and Matsue Plain, Shimane Prefecture, *JSCE Journal of Earthquake Engineering*, Vol.65, No.1, 97-103 (in Japanese with English abstract)

